Comparison of breakup processes of ^{6}He and ^{6}Li with four-body CDCC

[1]*Shin Watanabe,* [1]*Takuma Matsumot,* [1]*Kosho Minomo,* [2]*Kazuyuki Ogata, and* [1]*Masanobu Yahiro*
[1]Kyushu University, Fukuoka, Japan,
[2]RCNP, Osaka University, Osaka, Japan

Abstract
We have investigated projectile breakup effects on ^{6}Li+^{209}Bi elastic scattering near the Coulomb barrier with the four-body version of the continuum-discretized coupled-channels method. In this analysis, the elastic scattering is well described by the p + n + ^{4}He + ^{209}Bi four-body model. Four-body dynamics of the elastic scattering is precisely investigated, and we then propose a reasonable d + ^{4}He + ^{209}Bi three-body model for describing the four-body scattering. This work is based on the article Phys. Rev. C **86**, 031601(R) (2012).

1 Introduction

The Continuum-Discretized Coupled Channels method (CDCC) is a fully quantum-mechanical method of describing not only three-body scattering but also four-body scattering [1–3]. We call CDCC for four-body (three-body) scattering four-body (three-body) CDCC. CDCC has succeeded in reproducing experimental data on both three- and four-body scattering [4–13].

^{6}He + ^{209}Bi scattering near the Coulomb barrier was analyzed with three-body CDCC [14]. Reference [14] based on a ^2n + ^{4}He + ^{209}Bi three-body model; that is to say a pair of extra neutrons in ^{6}He was treated as a single particle, dineutron (^2n). The three-body CDCC calculation, however, does not reproduce the angular distribution of the measured elastic cross section and overestimates the measured total reaction cross section by a factor of 2.5. This problem has been solved by four-body CDCC in which the total system is assumed to be a $n + n +$ ^{4}He + ^{209}Bi four-body system [10]. On the other hand, ^{6}Li + ^{209}Bi scattering has been analyzed only with three-body CDCC by assuming a d + ^{4}He + ^{209}Bi three-body model [14] (see Fig. 1 (a)). However, the calculation could not reproduce the data without normalization factors for the potential between ^{6}Li and ^{209}Bi. These studies strongly suggest that ^{6}Li + ^{209}Bi scattering should also be treated with four-body CDCC as well as ^{6}He + ^{209}Bi scattering.

In this work, we analyze ^{6}Li + ^{209}Bi elastic scattering at 29.9 and 32.8 MeV with four-body CDCC by assuming the p + n + ^{4}He + ^{209}Bi four-body model (see Fig. 1 (b)). This is the first application of four-body CDCC to ^{6}Li scattering. We deal with four-body dynamics of the elastic scattering explicitly, and propose a reasonable d + ^{4}He + ^{209}Bi three-body model for describing the four-body scattering.

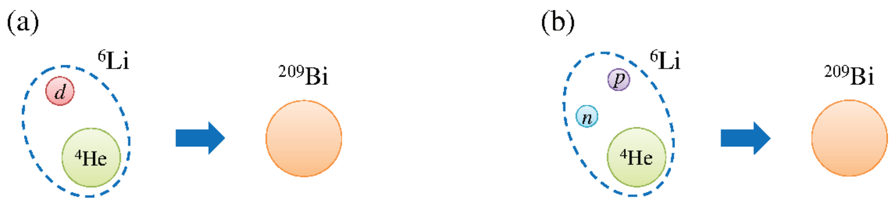

Fig. 1: (Color online) Schematic picture of three- and four-body systems. (a) represents d + ^{4}He + ^{209}Bi three-body model, and (b) represents p + n + ^{4}He + ^{209}Bi four-body model.

2 Theoretical framework

One of the most natural frameworks to describe ^{6}Li + ^{209}Bi scattering is the p + n + ^{4}He + ^{209}Bi four-body model. Dynamics of the scattering is governed by the Schrödinger equation

$$(H - E)\Psi = 0 \tag{1}$$

for the total wave function Ψ, where E is a total energy of the system. The total Hamiltonian H is defined by

$$H = K_R + U + h \tag{2}$$

with

$$U = U_n(R_n) + U_p(R_p) + U_\alpha(R_\alpha) + \frac{e^2 Z_{\rm Li} Z_{\rm Bi}}{R}, \tag{3}$$

where h denotes the internal Hamiltonian of ^{6}Li, $\boldsymbol{R}$ is the center-of-mass coordinate of ^{6}Li relative to ^{209}Bi, K_R stands for the kinetic energy operator associated with $\boldsymbol{R}$, and U_x describes the nuclear part of the optical potential between x and ^{209}Bi as a function of the relative coordinate R_x (see Fig. 2). As U_α, we adopt the optical potential of Barnett and Lilley [15]. Parameters of U_n are fitted to reproduce experimental data on n + ^{209}Bi elastic scattering at 5 MeV [16], where only the central interaction is taken for simplicity. The proton optical potential U_p is assumed to be the same as U_n. In the n + p + ^{4}He three-cluster model, we have numerically confirmed that the dipole strength is negligibly small. So, we can approximate the Coulomb part of p-^{209}Bi and α-^{209}Bi interactions into $e^2 Z_{\rm Li} Z_{\rm Bi}/R$, as shown in Eq. (3); $Z_{\rm A}$ is the atomic number of the nucleus A.

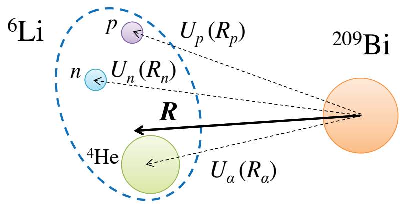

Fig. 2: (Color online) Illustration of coordinates of ^{6}Li + ^{209}Bi four-body system.

The internal Hamiltonian h of ^{6}Li is described by the p + n + ^{4}He orthogonality condition model [17]. The Hamiltonian of ^{6}Li agrees with that of ^{6}He in Ref. [10], when the Coulomb interaction between p and ^{4}He is neglected. Namely, the Bonn-A interaction [18] is taken in the p-n subsystem and the so-called KKNN interaction [19] is used in the p-α and n-α subsystems, where the KKNN interaction is determined from experimental data on low-energy nucleon-α scattering. In order to reproduce the measured binding energy of ^{6}Li, we introduce the effective three-body interaction. The calculated results for the ^{6}Li ground state are summarized in Table 1.

	I^π	ϵ_0 [MeV]	$R^{\rm m}_{\rm rms}$ [fm]
Calc.	1^+	-3.68	2.34
Exp.	1^+	-3.6989	2.44 ± 0.07

Table 1: Calculated spin-parity (I^π), energy (ϵ_0) and matter radius ($R^{\rm m}_{\rm rms}$) of the ^{6}Li ground state. The experimental data are taken from Refs. [20,21].

Eigenstates of h consist of finite number of discrete states with negative energies and continuum states with positive energies. In four-body CDCC, the continuum states of projectile are discretized into a finite number of pseudostates by either the pseudostate method [4–12] or the momentum-bin method [13]. The Schrödinger equation (1) is solved in a model space $\mathcal{P}$ spanned by the discrete and discretized-continuum states:

$$\mathcal{P}(H-E)\mathcal{P}\Psi_{\rm CDCC}=0. \tag{4}$$

In the pseudostate method, the discrete and discretized continuum states are obtained by diagonalizing h in a space spanned by L^2-type basis functions. As the basis function, the Gaussian [5–7, 10] or the transformed Harmonic Oscillator function [4, 8, 9, 11, 12] is usually taken. In this paper, we use the Gaussian function. The model space $\mathcal{P}$ is then described by

$$\mathcal{P} \;=\; \sum_{nIm}|\Phi_{nIm}\rangle\langle\Phi_{nIm}|, \tag{5}$$

where Φ_{nIm} is the nth eigenstate of ^{6}Li with an energy ϵ_{nI}, a total spin I and its projection on the z-axis m.

The CDCC wave function $\Psi^{JM}_{\rm CDCC}$, with the total angular momentum J and its projection on the z-axis M, are expressed as

$$\Psi^{JM}=\sum_{\gamma}\chi^J_\gamma(P_{nI},R)/R\,\mathcal{Y}^{JM}_\gamma \tag{6}$$

with

$$\mathcal{Y}^{JM}_\gamma=\Big[\Phi_{nI}(\boldsymbol{\xi})\otimes i^L Y_L(\hat{\boldsymbol{R}})\Big]_{JM} \tag{7}$$

for the orbital angular momentum L with respect to $\boldsymbol{R}$. Here $\boldsymbol{\xi}$ is a set of internal coordinates of ^{6}Li and the expansion coefficient χ^J_γ, where $\gamma=(n,I,L)$, describes a motion of ^{6}Li in its (n,I) state with linear momentum P_{nI} relative to the target. Multiplying the four-body Schrödinger equation (4) by $\mathcal{Y}^{*JM}_{\gamma'}$ from the left and integrating it over all variables except R, one can obtain a set of coupled differential equations for χ^J_γ:

$$\left[\frac{d^2}{dR^2}-\frac{L(L+1)}{R^2}-\frac{2\mu}{\hbar^2}U_{\gamma\gamma}(R)+P^2_{nI}\right]\chi^J_\gamma(P_{nI},R)=\frac{2\mu}{\hbar^2}\sum_{\gamma'\neq\gamma}U_{\gamma'\gamma}(R)\chi^J_{\gamma'}(P_{n'I'},R) \tag{8}$$

with the coupling potentials

$$U_{\gamma'\gamma}(R)=\langle\mathcal{Y}^{JM}_{\gamma'}|U_n(R_n)+U_p(R_p)+U_\alpha(R_\alpha)|\mathcal{Y}^{JM}_\gamma\rangle+\frac{e^2Z_{\rm Li}Z_{\rm Bi}}{R}\delta_{\gamma'\gamma}, \tag{9}$$

where μ is the reduced mass between ^{6}Li and ^{209}Bi. The elastic and discrete breakup S-matrix elements are obtained by solving Eq. (8) under the standard asymptotic boundary condition [1, 22].

In order to obtain Φ_{nIm}, we assume $I^\pi=1^+,2^+$ and 3^+ states with isospin zero and diagonalize h with 10 Gaussian basis functions for each coordinate in which the range parameters are taken from 0.1 to 12 fm in a geometric series. As shown in Table 1, the calculated binding energy and the matter radius of the ^{6}Li ground state are in good agreement with the experimental data. The Φ_{nIm} with its eigenenergy $\epsilon_{nI}>20$ MeV are excluded from $\mathcal{P}$. The resulting numbers of discrete states are 64 (including the ground state of ^{6}Li), 56, and 57 for 1^+, 2^+, and 3^+ states, respectively. We have also confirmed numerically that other spin-parity states such as $I^\pi=0^+$ and negative parity states do not affect the present results. The model space thus obtained gives good convergence within 1% of the calculated elastic cross sections for the ^{6}Li + ^{209}Bi scattering at 29.9 and 32.8 MeV.

We also perform three-body CDCC calculations by assuming a d + ^{4}He + ^{209}Bi model, following Refs. [14, 23]. As an interaction between d and ^{4}He, we take the potential of Ref. [24], which was determined from experimental data on the ground-state energy (-1.47 MeV) and the 3^+-resonance state energy (0.71 MeV) of ^{6}Li and low-energy d-α scattering phase shifts. The continuum states between d and ^{4}He are discretized with the pseudostate method [5] and are truncated at 20 MeV in the excitation energy of ^{6}Li from the d-^{4}He threshold. The d-^{209}Bi optical potential ($U_d^{\rm OP}$) [25] is taken as U_d, i.e., the distorting potential between d and ^{209}Bi in a d + ^{4}He + ^{209}Bi three-body Hamiltonian, whereas U_α is common between three- and four-body CDCC calculations.

3 Results

Figure 3 shows the angular distribution of elastic cross section for ^{6}Li + ^{209}Bi scattering at 29,9 MeV and at 32.8 MeV. The dotted line shows the result of three-body CDCC calculation with $U_d^{\rm OP}$ as U_d. This result underestimates the measured cross section [26, 27]. The solid (dashed) line, meanwhile, stands for the result of four-body CDCC calculation with (without) projectile breakup effects. In CDCC calculations without ^{6}Li-breakup, the model space $\mathcal{P}$ is composed only of the ^{6}Li ground state. The solid line reproduces the experimental cross section, but the dashed line does not. The projectile breakup effects are thus significant and the present ^{6}Li scattering is well described by the p + n + ^{4}He + ^{209}Bi four-body model.

Now we consider d-breakup in the ^{6}Li scattering in order to understand four-body dynamics of the scattering. In the limit of no d-breakup, the interaction between d and ^{209}Bi can be obtained by folding U_n and U_p with the deuteron density. This potential is referred to as the single-folding potential $U_d^{\rm SF}$. Note that we use the same U_n and U_p as for four-body CDCC (see Eq. 3). In Fig. 3, the dot-dashed line show the result of the three-body CDCC calculation with $U_d^{\rm SF}$ as U_d. The result well simulates that of four-body CDCC calculation, i.e., the solid line. This result suggests d-breakup is suppressed in the ^{6}Li scattering. Thus we found that the reason why three-body CDCC with $U_d^{\rm OP}$ does not work may be because we manage to count d-breakup, which is almost absent in d in ^{6}Li scattering.

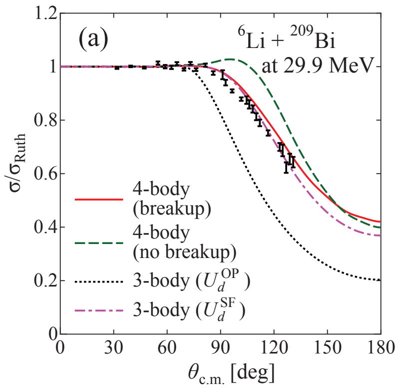

(i) ^{6}Li + ^{209}Bi scattering at 29.9 MeV

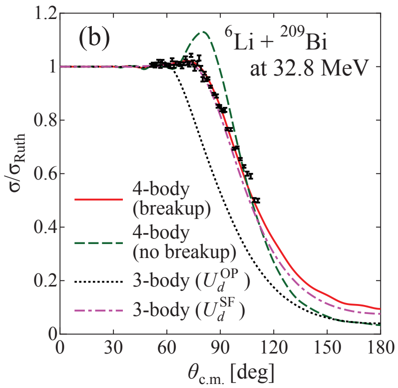

(ii) ^{6}Li + ^{209}Bi scattering at 32.8 MeV

Fig. 3: (Color online) Angular distribution of the elastic cross section for ^{6}Li + ^{209}Bi scattering at 29,9 MeV (a) and at 32.8 MeV (b). The cross section is normalized by the Rutherford cross section. The dotted (dot-dashed) line stands for the result of three-body CDCC calculation in which $U_d^{\rm OP}$ ($U_d^{\rm SF}$) is taken as U_d. The solid (dashed) line represents the result of four-body CDCC calculations with (without) breakup effects. The experimental data are taken from Refs. [26,27].

Figure 4 shows the angular distribution of elastic cross section for d + ^{209}Bi scattering at 12.8 MeV.

The solid and dashed lines stand for the results of three-body CDCC calculations with and without d-breakup, respectively, in which the $p + n +$ ^{209}Bi model is assumed and both Coulomb and nuclear breakup effects are taken into account. In this calculation, the discretized continuum states of d, obtained by the pseudostate method, are truncated at 30 MeV in the excitation energy from the n-p threshold. As the relative angular momentum ℓ between n and p, we take up to $\ell = 4$. The resulting number of discretized states is 13 (14) for $\ell = 0$ and 1 ($\ell = 2, 3$, and 4). The model space gives good convergence of the calculated elastic cross sections within 1%. The solid line reproduces the data fairly well, but the dashed line (one channel calculation with $U_d^{\rm SF}$) does not. Thus d-breakup is significant for the deuteron scattering. The deuteron optical potential $U_d^{\rm OP}$ (dotted line) yields fairly good agreement with the data, but the imaginary part of $U_d^{\rm OP}$ is much larger than that of $U_d^{\rm SF}$ mainly because of d-breakup effects. This is the reason why three-body CDCC calculations with $U_d^{\rm OP}$ as U_d cannot reproduce the measured elastic cross section for ^{6}Li + ^{209}Bi scattering. $U_d^{\rm OP}$ implicitly includes d-breakup effects, which is almost absent in d in ^{6}Li scattering.

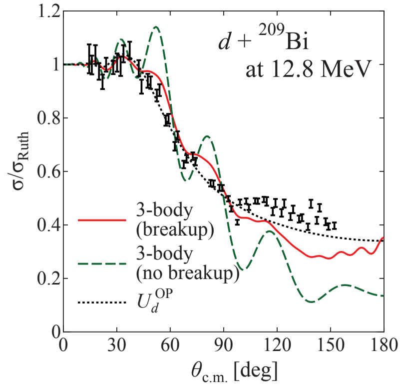

Fig. 4: (Color online) Angular distribution of the elastic cross section for d + ^{209}Bi scattering at 12.8 MeV. The solid (dashed) line stands for the result of three-body CDCC calculation with (without) deuteron breakup, whereas the dotted line is the result of the deuteron optical potential $U_d^{\rm OP}$. The experimental data are taken from Ref. [25].

4 Summary

The ^{6}Li + ^{209}Bi scattering at 29.9 MeV and 32.8 MeV near the Coulomb barrier is well described by four-body CDCC based on the $p + n +$ ^{4}He + ^{209}Bi model. This is the first application of four-body CDCC to ^{6}Li scattering. In the ^{6}Li scattering, d-breakup is strongly suppressed, suggesting that the d + ^{4}He + ^{209}Bi model becomes good, if the single-folding potential $U_d^{\rm SF}$ with no d-breakup is taken as an interaction between d and the target. For d+ ^{209}Bi scattering at 12.8 MeV, meanwhile, d-breakup is significant, so that the deuteron optical potential $U_d^{\rm OP}$ includes d-breakup effects. That is to say, the failure of three-body CDCC with $U_d^{\rm OP}$ may be because we manage to count d-breakup, which is almost absent in d in ^{6}Li scattering. However, we need to discuss carefully whether we can always neglect d-breakup in ^{6}Li. We will investigate the energy and target dependence of d-breakup effects in ^{6}Li scattering.

The authors would like to thank Y. Watanabe, K. Kato, and Y. Hirabayashi for helpful discussions. This work has been supported in part by the Grants-in-Aid for Scientific Research of Monbukagakusho of Japan and JSPS.

References

[1] M. Kamimura, M. Yahiro, Y. Iseri, Y. Sakuragi, H. Kameyama, and M. Kawai, Prog. Theor. Phys. Suppl. **89**, 1 (1986).

[2] N. Austern, Y. Iseri, M. Kamimura, M. Kawai, G. Rawitscher, and M. Yahiro, Phys. Rep. **154**, 125 (1987).

[3] M. Yahiro, K. Ogata, T. Matsumoto, and K. Minomo, M. Yahiro, K. Ogata, T. Matsumoto, and K. Minomo, Prog. Theor. Exp. Phys. 2012, 01A206 (2012).

[4] A. M. Moro, J. M. Arias, J. Gómez-Camacho, I. Martel, F. Pérez-Bernal, R. Crespo, and F. Nunes, Phys. Rev. C **65**, 011602(R) (2001).

[5] T. Matsumoto, T. Kamizato, K. Ogata, Y. Iseri, E. Hiyama, M. Kamimura, and M. Yahiro, Phys. Rev. C **68**, 064607 (2003).

[6] T. Matsumoto, E. Hiyama, K. Ogata, Y. Iseri, M. Kamimura, S. Chiba, and M. Yahiro, Phys. Rev. C **70**, 061601(R) (2004).

[7] T. Egami, K. Ogata, T. Matsumoto, Y. Iseri, M. Kamimura, and M. Yahiro, Phys. Rev. C **70**, 047604 (2004).

[8] M. Rodríguez-Gallardo, J. M. Arias, J. Gómez-Camacho, A. M. Moro, I. J. Thompson, and J. A. Tostevin, Phys. Rev. C **72**, 024007 (2005).

[9] A. M. Moro, F. Pérez-Bernal, J. M. Arias, and J. Gómez-Camacho, Phys. Rev. C **73**, 044612 (2006).

[10] T. Matsumoto, T. Egami, K. Ogata, Y. Iseri, M. Kamimura, and M. Yahiro, Phys. Rev. C **73**, 051602(R) (2006).

[11] M. Rodríguez-Gallardo, J. M. Arias, J. Gómez-Camacho, R. C. Johnson, A. M. Moro, I. J. Thompson, and J. A. Tostevin, Phys. Rev. C **77**, 064609 (2008).

[12] A. M. Moro, J. M. Arias, J. Gómez-Camacho, and F. Pérez-Bernal, Phys. Rev. C **80**, 054605 (2009).

[13] M. Rodríguez-Gallardo, J. M. Arias, J. Gómez-Camacho, A. M. Moro, I. J. Thompson, and J. A. Tostevin, Phys. Rev. C **80**, 051601(R) (2009).

[14] N. Keeley, J. M. Cook, K. W. Kemper, B. T. Roeder, W. D. Weintraub, F. Maréchal, and K. Rusek, Phys. Rev. C **68**, 054601 (2003).

[15] A. R. Barnett and J. S. Lilley, Phys. Rev. C **9**, 2010 (1974).

[16] J. Annand, R. Finlay, and P. Dietrich, Nuclear Physics A **443**, 249 (1985).

[17] S. Saito, Prog. Theor. Phys. **41**, 705 (1969).

[18] R. Machleidt, Adv. Nucl. Phys. **19**, 189 (1989).

[19] H. Kanada, T. Kaneko, S. Nagata, and M. Nomoto, Prog. Theor. Phys. **61**, 1327 (1979).

[20] D. R. Tilley *et al.*, Nucl. Phys. A **708**, 3 (2002).

[21] A. V. Dobrovolsky *et al.*, Nucl. Phys. A **766**, 1 (2006).

[22] R. A. D. Piyadasa, M. Yahiro, M. Kamimura, and M. Kawai, Prog. Theor. Phys. **81**, 910 (1989).

[23] K. Rusek, I. Martel, J. Gómez-Camacho, A. M. Moro, and R. Raabe, Phys. Rev. C **72**, 037603 (2005).

[24] Y. Sakuragi, M. Yahiro, and M. Kamimura, Prog. Theor. Phys. Suppl. **89**, 136 (1986).

[25] A. Budzanowski, L. Freindl, K. Grotowski, M. Rzeszutko, M. Słapa, J. Szmider, and P. Hodgson, Nuclear Physics **49**, 144 (1963).

[26] E. F. Aguilera *et al.*, Phys. Rev. Lett. **84**, 5058 (2000).

[27] E. F. Aguilera *et al.*, Phys. Rev. C **63**, 061603 (2001).